Tomographic computational tool for concrete discontinuities identification using ultrasonic testing with synthetic data

Ferramenta informática tomográfica para identificação de descontinuidades do betão utilizando testes ultra-sónicos com dados sintéticos

Laio Andrade Sacramento
Especialista
Universidade Estadual de Santa Cruz (UESC) – Programa de Pós-Graduação em Modelagem Computacional em Ciência e Tecnologia (PPGMC)
Instituição: Universidade Estadual de Santa Cruz, Campus Soane Nazaré de Andrade
Endereço: Rodovia Jorge Amado, km 16, Bairro Salobrinho, CEP 45662-900. Ilhéus-Bahia.
E-mail: lasacramento@uesc.br

Dany Sanchez Dominguez
Doutor
Universidade Estadual de Santa Cruz (UESC) – Programa de Pós-Graduação em Modelagem Computacional em Ciência e Tecnologia (PPGMC)
Instituição: Universidade Estadual de Santa Cruz, Campus Soane Nazaré de Andrade
Endereço: Rodovia Jorge Amado, km 16, Bairro Salobrinho, CEP 45662-900. Ilhéus Bahia
E-mail: dsdominguez@uesc.br

José Renato de Castro Pessôa
Doutor
Universidade Estadual de Santa Cruz (UESC) – Programa de Pós-Graduação em Modelagem Computacional em Ciência e Tecnologia (PPGMC)
Instituição: Universidade Estadual de Santa Cruz, Campus Soane Nazaré de Andrade
Endereço: Rodovia Jorge Amado, km 16, Bairro Salobrinho, CEP 45662-900. Ilhéus-Bahia
E-mail: jrcpessoa@uesc.br

Susana Marrero Iglesias
Doutora
Universidade Estadual de Santa Cruz (UESC) – Programa de Pós-Graduação em Modelagem Computacional em Ciência e Tecnologia (PPGMC)
Instituição: Universidade Estadual de Santa Cruz, Campus Soane Nazaré de Andrade, Rodovia Jorge
Endereço: Amado, km 16, Bairro Salobrinho, CEP 45662-900. Ilhéus-Bahia.
E-mail: smiglesias@uesc.br

ABSTRACT

The presence of pathologies in concrete structures is a major problem for civil engineering, in particular when they are not located on the object surface. In this regard, digital tomographic reconstruction techniques have proved to be a great ally for the study of the internal structure of materials. Thus, this work aims to develop a computational tool combining tomographic techniques with the ultrasonic pulse velocity test to identify non-homogeneities within concrete structures. With this aim, the essential mathematical background for a better understanding of the tomographic problem, and the necessary steps for computational implementation are presented. The tomographic reconstruction algorithm was implemented in MatLab. To verify the effectiveness of the developed code, six simulated specimens were used representing internal sections of elements with discontinuities of different sizes and locations. Pulse propagation time vectors have been developed for horizontal, vertical, and composite reading configurations. To study the mesh dependency, meshes of 5cm x 5cm and 2.5cm x 2.5cm were used. The developed algorithm was able to create tomograms of the internal structure of the proposed elements. The results obtained both in terms of location and dimensioning of the discontinuities were best represented by the 2.5cm x 2.5cm mesh.

Keywords: Concrete Inspection, Non-Destructive Evaluation, Ultrasonic Pulse Velocity, Tomography.

RESUMO

A presença de patologias em estruturas de betão é um grande problema para a engenharia civil, em particular quando estas não estão localizadas na superfície do objecto. A este respeito, as técnicas de reconstrução tomográfica digital provaram ser um grande aliado para o estudo da estrutura interna dos materiais. Assim, este trabalho visa desenvolver uma ferramenta computacional que combina técnicas tomográficas com o teste de velocidade de pulso ultra-sónico para identificar não-homogeneidades dentro de estruturas de betão. Com este objectivo, são apresentados os antecedentes matemáticos essenciais para uma melhor compreensão do problema tomográfico, e os passos necessários para a implementação computacional. O algoritmo de reconstrução tomográfica foi implementado no MatLab. Para verificar a eficácia do código desenvolvido, foram utilizados seis exemplares simulados representando secções internas de elementos com descontinuidades de diferentes tamanhos e localizações. Foram desenvolvidos vectores de tempo de propagação de pulso para configurações de leitura horizontal, vertical, e composta. Para estudar a dependência da malha, foram utilizadas malhas de 5cm x 5cm e 2,5cm x 2,5cm. O algoritmo desenvolvido foi capaz de criar tomogramas da estrutura interna dos elementos propostos. Os resultados obtidos tanto em termos de localização como de dimensionamento das descontinuidades foram melhor representados pela malha de 2,5cm x 2,5cm.

Palavras-Chave: Inspecção Concreta, Avaliação não Destrutiva, Velocidade de Pulso Ultra-Sónico, Tomografia.

1 INTRODUCTION

The interest in studying the integrity of concrete structures is the focus of numerous researches in civil engineering (Pessôa et al. 2016; Reginato et al. 2017a; Haach and Ramirez 2016). Differences in homogeneity, degradation over time, exposure to harmful environments, loading cracking, presence of voids or strange bodies are some of the pathologies that can be developed in these structures (Pessoa 2011; Souza and Ripper 2009; Meira et al. 2020).

In this sense, non-destructive evaluation can be used to characterize properties and pathologies in concrete structures without affecting their visual aspect or integrity. In particular, the ultrasonic pulse velocity test can be used to inspect the internal integrity of structures (Lopes 2014; Reginato et al. 2017a).

Even being able to evaluate the general conditions of homogeneity in concrete, the ultrasonic pulse velocity test alone is not able to locate and dimension internal discontinuities in the structures. Therefore, combining the traditional ultrasonic test with a tomographic reconstruction algorithm is an alternative to solve this problem (Perlin 2015).

The ultrasonic tomography is a non-destructive evaluation method that combines a tomographic algorithm with ultrasonic readings in several directions to reconstruct internal sections of concrete bodies. (Choi and Popovics 2015; Haach and Ramirez 2016). In this regard, researches have been constantly directed towards the study, development, and improvement of tomographic algorithms for ultrasonic pulse inspection. The implementation of the algorithm, evaluation of solution methods for the tomographic equations system, data allocation, and solution for pre-established simplifications are some of the study topics (Haach and Ramirez 2016; Perlin and Pinto 2019; Perlin 2015).

Hence, the aim of this work is to describe the physical problem involving ultrasonic tomography, the characteristics of the developed equations systems, and to propose the implementation of an algorithm for its numerical solution.

2 BASIS OF ULTRASONIC TOMOGRAPHY

In a simplified way, the physical problem that governs the tomography is described in Fig1. The difference between the signal that leaves the source and arrives at the receiver provides the information about the interior structure of the body.

Considering projections in many different directions, it is possible to reconstruct the internal characteristics of the body (De Pierro 1990).

Figure 1 – Scheme of the physical principle that governs tomography.
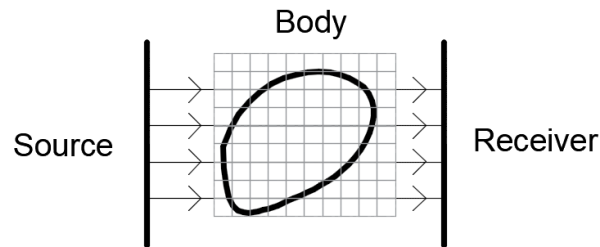
This is the basis of tomography and it can be expressed mathematically in the form

$$\Delta S = \int d_j a_j \tag{1}$$

where ΔS is the difference between the emitted and received signal, d_j é is the distance traveled by the signal in the infinitesimal element j, and a_j is the attenuation in the element.

In the ultrasonic tomography in concrete, the difference between the emitted and the received signal ΔS is the time T necessary for the ultrasonic pulse to be emitted from the emitting transducer, to pass-through the concrete body and to be received at the receiving transducer. The attenuation property a_j is the resistance that the material has in relation to the wave propagation velocity, and this can be expressed as

$$p = \frac{1}{V} \tag{2}$$

where p is known as pulse vagarosity, and V is the ultrasonic pulse velocity.

The elements d_j refer to the geometry of the body and mesh discretization. Thus, the equation that describes the travel time of the ultrasonic pulse in the concrete can be expressed as

$$T = \int_e^r p_j dL_j \tag{3}$$

where T is the travel time, p_j is the pulse vagarosity in element j, and dL_j is the traveled distance in element j.

The integral described in Eq. 3 can be numerically approximated for a summation using numerical quadrature methods (Burden and Faires 2011). Thus, the approximate integral that describes the travel time of the ultrasonic pulse in the concrete can be write as

$$T_i = \sum_{j=1}^{n} p_j dL_{i,j} \qquad \text{for } i = 1, \dots, m \qquad (4)$$

where i represents each ultrasonic test trajectories. Equation 4 can be represented in matrix form as

$$T_m = D_{m,n} * P_n \qquad (5)$$

where m is the total number of pulse readings, n is the total number of discretized elements inside the body, D is the distance matrix of order m x n, P is the slowness vector of order n, and T is the time vector of order m.

It is noticed that the time vector is obtained through the readings of the ultrasonic pulse velocity test, and the distance matrix is calculated from the geometric characteristics of the body and the established mesh. Then, the ultrasonic tomographic problem is reduced to determining the vagarosity vector.

3 EXPERIMENTAL PROGRAM

3.1 DEVELOPMENT OF A TOMOGRAPHIC TOOL

For computational development, the described mathematical basis was used. Figure 2 illustrates the steps used in the implementation. The inputs used were the geometric characteristics of the problem to create the distance matrix $D_{m,n}$, and the vector of synthetic time readings T_m. The output is the tomogram that represents the internal section of the simulated object.

Step 1 refers to the data entry of the geometric characteristics of the studied section (height and width). The tomographic process requires the body to be discretized into smaller elements where the numerical operations will be computed. Thus, step 2 of Fig. 2, refers to the mesh definition on the studied element, the positioning of the transducers, and the reading trajectories definition.

The data entry of the time vector T_m is performed in step 3 of Fig. 2. In this stage of the work, the data entry will be done through the use of synthetic data. The

creation of these data, application criteria, and what they simulate are described in section 3.2 Experimental Program: Creation of time vectors.

Figure 2 – Diagram of the computational implementation process.
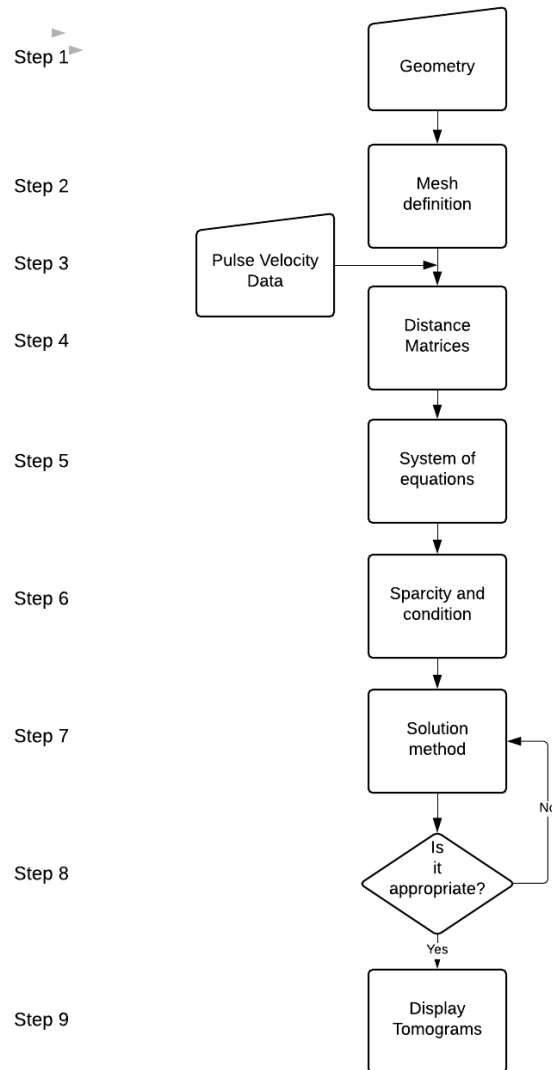
Once the mesh has been determined, the positions of the transducers, the sections of readings and their lengths, we can proceed to step 4 of Fig. 2, referring to the construction of the distance matrix. In addition to knowing the information about the position of the transducers and the length of the section, it is necessary to compute how much of the reading path goes through each of the discretized elements in the body.

Now that we know the time vector and the distance matrix is calculated, the tomographic system can be set up. Step 5 in Fig. 2 is responsible for this procedure. In step 6 of Fig. 2, the sparsity and condition analyzes are performed. At this stage, we study the structure of the elements of the system of equations to choose the best solution method.

Now that we know the components of the system of equations and the characteristics of the distance matrix, we proceed to step 7, the implementation of a solution method. In this stage of the work, the following solution methods will be used: 1- LU factorization with partial pivoting if the distance matrix is square; or QR factorization with column pivoting for other cases.

The obtained result is evaluated in step 8. This step is iterative once, depending on the found results, it is needed to repeat step 7 using a new solution method. Two evaluations must be made to assess the efficiency of the solution method. The first is to verify whether the method can effectively solve the proposed system. The second is related to the methods that effectively manage to solve the system, and consists of verifying if the precision of the obtained result is in agreement with the user's need.

Finally, step 9 in Fig. 2, consists of displaying the vagarosity vector to the user as a tomogram. For that, we use the contour maps representation. Contour maps are already used for the traditional representation of ultrasonic pulse evaluations on concrete.(RIBEIRO et al. 2020; Reginato et al. 2017b).

3.2 CREATION OF TIME VECTORS

In order to verify the capacity of the algorithm of developing tomograms, we had chosen the construction of synthetic data of ultrasound readings.

The ultrasonic pulse velocity readings in concrete specimens are affected by numerous factors, such as lack of accuracy of the inspector, reading angle, poor transducers coupling, piece surface conditions, among others (Malhotra and Carino 2004; Mohammed and Rahman 2016; GODINHO et al. 2020; Perlin 2015). Thus, the option for synthetic data was made to guarantee control over the results in this stage of the tool efficiency testing.

We created a virtual specimen (VS) with dimensions of 15cm x 15cm, and we assign characteristics of a fictitious homogeneous material, which means, the ultrasonic pulse velocity does not vary while passing through the same material. We attribute to this material an ultrasonic pulse velocity equal to 1 m/s.

To assess the capacity of the algorithm for detecting internal discontinuities in the material and generating the tomogram, elements of 5cm x 5cm x 5cm and 2.5cm x 2.5cm x 2.5cm were located inside the body in different configurations. To ensure discrepancy between the discontinuity pulse velocity and the base material, we assign a pulse velocity of 0,5m/s to the discontinuity.

To verify the mesh dependency of the developed algorithm, two meshes were used. The first mesh with a grid of 5cm x 5cm, following the dimensions of the largest simulated discontinuities, and the second mesh of 2.5cm x 2.5cm.

For better understanding, the following nomenclature was attributed to the developed VSs. First we relate the property of the mesh, 5cm x 5cm (m50), or 2.5cm x 2.5cm (m25). Then the type of reading, which can be horizontal (h), vertical (v), or compound (hv). Next, the discontinuity dimension of 50mm x 50mm (50), or 25mm x 25mm (25). And finally, the location of the discontinuity in the body, which is centered (ce), lower-left corner (ie), or main diagonal (sd). Figure 3 shows the geometric domain of a virtual specimen.

Figure 3 – Virtual specimens. a) m50hv50ce, b) m50hv50ie, c) m50hv50dp, d) m50hv25ce, e) m50hv25ie e f)m50hv25dp.
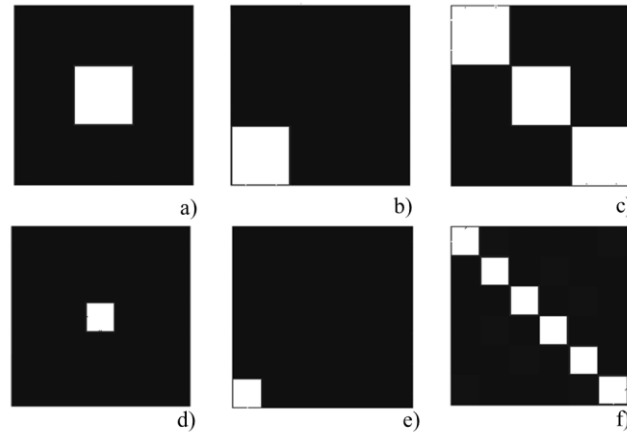
The elaboration of the time vectors was performed by calculating, for each reading, the component parts of the traveled pulse in the discretized mesh, and weighting by 1m/s for sections through the base material and 0.5m/s for sections through the discontinuities.

The capacity to generate tomographic images of the algorithm developed based on reading directions was also evaluated. Then, the time vector was composed of simulated readings in the horizontal direction, in the vertical direction and simultaneously in both directions.

## 4 RESULTS AND DISCUSSION

4.1 DISTANCE MATRICES

The distance matrices were calculated according to that described in previous sections. Since they describe purely the geometric characteristics of the path in the discretized mesh, 6 different matrices were obtained and can be used for the set of readings. Figure 4 shows the meshes and reading paths used for creating the distance matrices.

The analysis of Fig. 4 is as a good device to verify the operation of the algorithm in the calculation of distance matrices. From it, we can observe that: 1- the reading grid was properly discretized; 2- the intersections between the readings and the grid lines were properly established; 3- there are no reading paths outside the domain that are being computed in the matrix; 4- the location of the reading sections in the distance matrix $D_{m,n}$ is correct.

It is also noticed that in Figure 4 (c) and (f), the density of reading passing through each mesh element is visibly higher than in the horizontal and vertical readings only. The impact of different reading configurations on the final tomogram will be discussed in the following sections.

Figure 4- Reading paths. For the 5cm x 5cm mesh: horizontal readings (a), vertical readings (b), composed readings (c). For the 2.5cm x 2.5cm mesh: horizontal readings (d), vertical readings (e), composed readings (f).
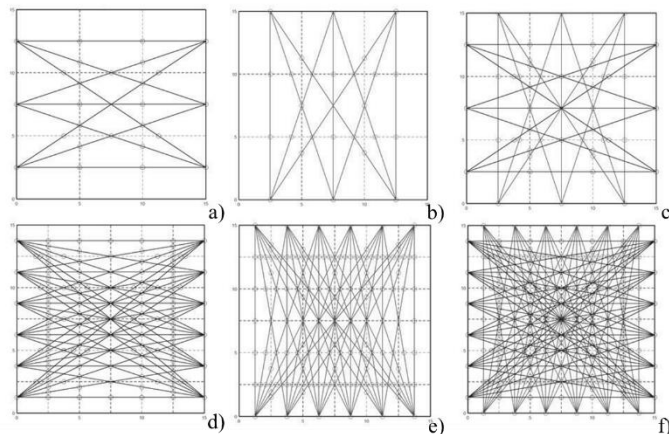
4.2 SPARCITY AND CONDITION

An analysis of sparsity, condition, and order of the distance matrices was performed as a way to study the behavior of the developed systems of equations. The results obtained can be seen in Table 1.

Table 1 – Order, condition and sparcity for each distance matrix.

Mesh	Order	Condition	Sparcity (%)
50x50h	9X9	$2.61*10^{16}$	56.79
50x50v	9X9	$1.67*10^{16}$	56.79
50x50hv	18X9	3.2074	56.79
25x25h	36X36	$1.46*10^{17}$	80.25
25x25v	36X36	$4.56*10^{17}$	80.25
25x25hv	72X36	10.1328	80.25

Table 2 shows that the distance matrices generated from readings in one direction are square, which provides us linear equations systems without overdetermination. Overdetermination is a characteristic of the matrices generated in the 50x50hv and 25x25hv meshes.

The difference between the condition of the matrices is also evident. The matrices generated from composite readings have a low condition number, while the other matrices have it way higher. High conditioning numbers can be indicative of distance matrix singularity.

Regarding sparsity, it is clear that regardless of the mesh, the problem is composed of sparse matrices. This number indicates that for 5cm x 5cm meshes 56.79% of the terms in the distance matrix are null, while this value reaches 80.25% for 2.5cm x 2.5cm meshes.

Therefore, it may be noted from the characteristics of the calculated distance matrices that the tomographic problem in question can be divided into two groups: 1- overdetermined, well-conditioned systems with a high degree of sparsity; and 2- systems without overdetermination, poorly conditioned and also sparse.

4.3 TOMOGRAMS

With the distance matrices properly computed, and time vectors inserted, the algorithm solved the systems of equations and delivered the numerical results. The tomograms were generated from contour images, by linear interpolation of the results obtained and are shown in Fig. 5 and 6.

In this work, we focused on the solution of the systems generated from composite readings (Fig. 4 (c) and (f)) of overdetermined, sparse, and well conditioned systems. For the solution of poorly conditioned systems, Perlin (2015) indicates the numerical solution method by optimized Cimmino or Karczmarz.

Figure 5- Generated tomograms for the 5cm x 5cm mesh. a) m50hv50ce, b) m50hv50ie, c) m50hv50dp, d) m50hv25ce, e) m50hv25ie e f)m50hv25dp.
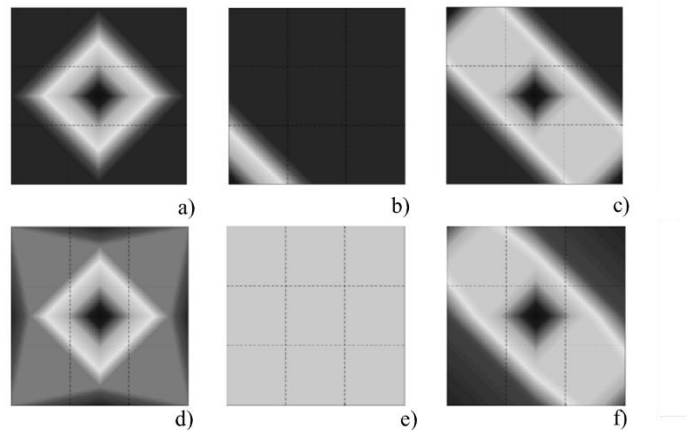
In general, the proposed algorithm was able to represent the location of internal discontinuities in the 5cm x5cm mesh (Fig. 5), except in the VP m50hv25ie tomogram. The non-representation of the 2.5cm x 2.5cm defect in the lower-left corner by the 5cm x 5cm mesh (Fig. 5 (e)) was observed, and can be explained since no component of the reading vector crosses the discontinuity. For this mesh, the geometric characteristics of the discontinuities do not represent their nature.

Figure 6- Generated tomograms for the 2.5cm x 2.5cm. a) m25hv50ce, b) m25hv50ie, c) m25hv50dp, d) m25hv25ce, e) m25hv25ie e f) m25hv25dp.
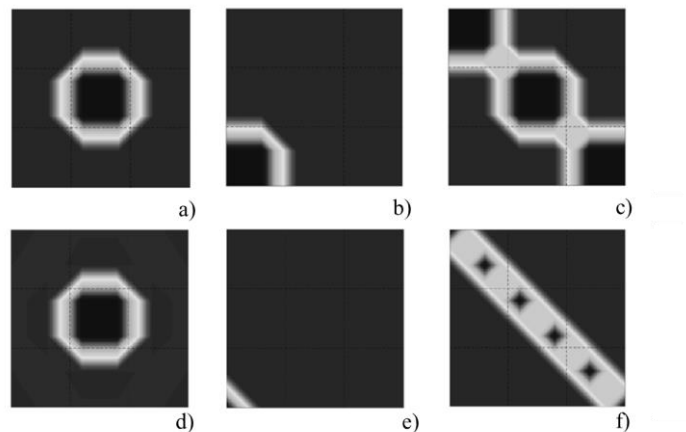
With the mesh reduction to 2.5cm x 2.5cm, we continue to notice the ability of the algorithm to identify the location of discontinuities in the material. Regarding its geometric nature, it was noticed that in all cases the decrease in the mesh led to a better quality of the final result, which was expected by the characteristics of the problem. The greater the number of discretized elements, the greater the quality of the generated tomogram. However, it is warned that the gradual decrease of the mesh element by the

user must take into account the significant increase in the number of experimental readings, which can make the inspection impossible in practical terms.

5 CONCLUSIONS

In this work, we present the mathematical basis that involves the problem of ultrasonic tomography in concrete, the characteristics of the generated equation systems, and we proposed the implementation of an algorithm for its solution.

From the analysis of the generated systems and the resulting tomograms, we can conclude that:

- The problem of ultrasonic tomography can be divided into two major groups: poorly conditioned, square and sparse systems, and well-conditioned, over-determined and sparse systems;

- It was possible to present a solution method for sparse, well-conditioned, and over-determined tomographic problems, capable of generating tomograms of the internal structure of the material;

- Mesh dependence has a significant influence on the geometric representation of the internal defect. Smaller meshes lead to better tomograms.

 The future developments of this research suggest the implementation of the optimized Cimmino and Karczmarz methods to evaluate the algorithm in the solution of poorly conditioned systems. Also, evaluate the performance of the developed algorithm with time vector data generated from physical readings of ultrasonic pulse in concrete controlled samples.

REFERENCES

Burden, Richard L.;, and J. Douglas Faires. 2011. Numerical Analysis. 9th ed. Boston: Brooks/Cole.

Choi, Hajin, and John S. Popovics. 2015. "NDE Application of Ultrasonic Tomography to a Full-Scale Concrete Structure." IEEE Transactions on Ultrasonics, Ferroelectrics, and Frequency Control 62 (6): 1076–85. https://doi.org/10.1109/TUFFC.2014.006962.

GODINHO, J. P., T. F. DE SOUZA JÚNIOR, M. H. F. MEDEIROS, and M. S. A SILVA. 2020. "Factors Influencing Ultrasonic Pulse Velocity in Concrete." Revista IBRACON de Estruturas e Materiais 13 (2): 222–47. https://doi.org/10.1590/s1983-41952020000200004.

Haach, Vladimir G., and Fernando C. Ramirez. 2016. "Qualitative Assessment of Concrete by Ultrasound Tomography." Construction and Building Materials 119 (August): 61–70. https://doi.org/10.1016/j.conbuildmat.2016.05.056.

Lopes, Sergio Weber. 2014. "Avaliação Da Homogeneidade e Da Resistência à Compressão Do Concreto Por Meio de Ensaios Não Destrutivos." Universidade Federal de Viçosa.

Malhotra, V.M., and N.J. Carino. 2004. Handbook on Nondestructive Testing of Concrete. 2nd ed. West Conshohocken: CRC Press.

Meira, Suian Andrade, Laio Andrade Sacramento, Mariane Porto Lima, José Renato de Castro Pessôa, Flávia Lopes de Almeida Nascimento, and Joaquim Teixeira Assis. 2020. "Análise Da Porosidade de Concreto Por Processamento de Imagem: Uma Visão Da Sensibilidade Do Threshold Na Binarização." Brazilian Journal of Development 6 (3): 16449–59. https://doi.org/10.34117/bjdv6n3-497.

Mohammed, Tarek Uddin, and Md Nafiur Rahman. 2016. "Effect of Types of Aggregate and Sand-to-Aggregate Volume Ratio on UPV in Concrete." Construction and Building Materials 125 (October): 832–41. https://doi.org/10.1016/j.conbuildmat.2016.08.102.

Perlin, Lourenço Panosso. 2015. "Tomografia Ultrassônica Em Concreto e Madeira: Desenvolvimento de Ferramenta Computacional." Universidade Federal de Santa Catarina.

Perlin, Lourenço Panosso, and Roberto Caldas de Andrade Pinto. 2019. "Use of Network Theory to Improve the Ultrasonic Tomography in Concrete." Ultrasonics 96 (July): 185–95. https://doi.org/10.1016/j.ultras.2019.01.007.

Pessoa, Jose Renato de Castro. 2011. "CARACTERIZAÇÃO DE CONCRETO ENDURECIDO UTILIZANDO SCÂNER DE MESA E MICROTOMOGRAFIA COMPUTADORIZADA." Universidade do Estado do Rio de Janeiro.

Pessôa, José Renato de Castro, Dany Sanchez Dominguez, Joaquim Teixeira de Assis,

Marlesson Rodriguies Oliveira de Santana, and Leonardo Alves Dias. 2016. "Análise Volumétrica de Porosidade Do Concreto Através de Microtomografia Com Raio X e Processamento de Imagens." In XV Latin American Seminary of Analysis by X-Ray Techniques – SARX 2016, 18–21. Petrópolis.

Pierro, Alvaro R De. 1990. "Fundamentos Matemáticos Da Tomografia Computadorizada: Método de Transformação." Matemática Universitária 11: 53–65.

Reginato, Lucas Alexandre, Alexandre Lorenzi, Luciani Somensi Lorenzi, and Luiz Carlos Pinto da Silva Filho. 2017a. "Avaliação de Pilares de Concreto Armado Através de Ensaios de Pulso Ultrassônico." Revista de Engenharia Civil IMED 4 (1): 32. https://doi.org/10.18256/2358-6508/rec-imed.v4n1p32-47.

———. 2017b. "Avaliação de Pilares de Concreto Armado Através de Ensaios de Pulso Ultrassônico." Revista de Engenharia Civil IMED 4 (1): 47. https://doi.org/10.18256/2358-6508/rec-imed.v4n1p32-47.

RIBEIRO, Y. A. M., D. S. BOMFIM, L. A. SACRAMENTO, J. R. P. CASTRO, D. S. DOMINGUEZ, and M. P. LIMA. 2020. "IDENTIFICAÇÃO DE NÃO HOMOGENEIDADES EM ESTRUTURAS DE CONCRETO ENDURECIDO ATRAVÉS DE PULSO ULTRASSÔNICO." In >Congresso Brasileiro de Patologia Das Construções, 1329–38. Associação Brasileira de Patologia das Construções. https://doi.org/10.4322/CBPAT.2020.130.

Souza, Vicente Custódio de, and Thomaz Ripper. 2009. Patologia, Recuperação e Reforço de Estruturas de Concreto. 1st ed. São Paulo: Editora Pini Ltda.